ASSESSMENT OF THE HPLWR THERMAL CORE DESIGN

T. Schulenberg[1], C. Maráczy[2], W. Bernnat[3] and J. Starflinger[3]
[1] Karlsruhe Institute of Technology, Karlsruhe, Germany
[2] Hungarian Academy of Sciences KFKI, Budapest, Hungary
[3] IKE, University of Stuttgart, Germany

Abstract

The core design concept of the High Performance Light Water Reactor features a thermal neutron spectrum, provided by additional moderator water in water boxes and in gaps between assembly boxes, and a heat-up of the coolant in three steps from 280°C to 500°C. Intermediate coolant mixing has been foreseen by mixing chambers underneath and above the core to overcome the hot channel issue of a core design with a large enthalpy rise. The paper summarizes the various analyses performed within the project HPLWR-Phase 2 with respect to this core design and assesses how far the initial design target has been met.

1. Introduction

The High Performance Light Water Reactor is a conceptual design of a Supercritical Water Cooled Reactor, worked out from 2006 to 2010 by a consortium of 13 partners of 8 Euratom member states within the 6th European Framework Program as their contribution to the Generation IV International Forum. Starflinger et al. [1] summarize the HPLWR Phase 2 project and introduce the tasks of the project partners. Basically, the core of such a reactor can be designed with a thermal or fast neutron spectrum. Using synergies within the International Forum, however, the partners decided to concentrate mainly on a thermal core design, as will be described next, leaving the fast core studies to Japanese scientists, see Ishiwatari et al. [2].

2. HPLWR Thermal Core Design

2.1 Design Target

Aiming at a net electric power of around 1000MW and a net efficiency of almost 44%, the target thermal power of the reactor core needs to be 2300MW, confirmed by steam cycle analyses of Brandauer et al. [3]. Early cycle studies by Dobashi et al. [4] indicated an optimum thermal efficiency at a feedwater temperature of 280°C which was kept constant also for the present study. The target core outlet temperature was chosen as 500°C which is still rather low for a once through steam cycle with single reheat, compared with latest fossil fired power plants, but appears to be challenging enough with regard to available fuel cladding materials. Their peak temperature limit was targeted at 630°C which is not only a challenge for oxidation and corrosion protection, but also for their creep strength and resistance to stress corrosion cracking. The fuel centreline temperature is a function of the linear power of the fuel rod. The latter one has been limited to 39kW/m under nominal conditions. To be competitive with respect to latest pressurized water reactors, the target burn up should be at least 60 MWd/t_{HM}. Like with boiling water reactors, boron acid cannot be used to compensate the excess reactivity at the beginning of a burn-up cycle, so that burnable absorbers like Gd must be used instead. The target power and temperatures result in a coolant mass flow rate of 1179kg/s. Schlagenhaufer et al. [5] suggest a feedwater pressure of 25MPa for all load conditions which keeps some margin from the critical pressure of 22.1MPa.

2.2 General Design Strategy

These target data differ from conventional light water reactors not only by the higher pressure and core outlet temperature, but also by a significantly higher enthalpy rise in the core. Indeed, the difference between life steam enthalpy and feedwater enthalpy of 1936kJ/kg exceeds the one of pressurized water reactors by around a factor of 8. Assuming an overall hot channel factor of 2 between the peak and the average coolant heat-up, this enthalpy rise would result in peak coolant temperatures of 1200°C which is far beyond the target temperature limit. A strategy to overcome this issue can be learned from fossil fired boiler design. These boilers are characterized by multiple heat-up steps with intensive coolant mixing between them to eliminate hot streaks.

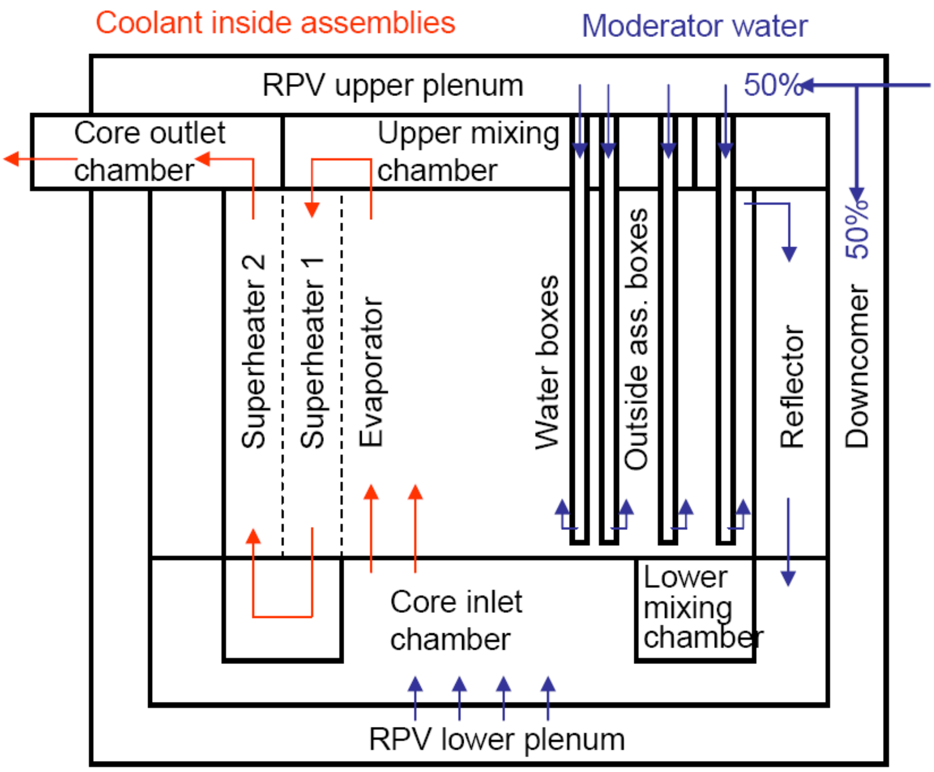

Figure 1 Sketch of the coolant flow path

Schulenberg et al. [6] applied such a strategy for a thermal core layout with a first heat-up of 50% of the coolant as moderator water, comparable with the economizer of a fossil fired boiler, as sketched in Figure 1. After mixing with the remaining feedwater, supplied through the downcomer, the second heat-up should be in the evaporator assemblies in the centre of the core, followed by coolant mixing in a mixing chamber above the core. From there, the coolant is directed downwards in assemblies of the first superheater, surrounding the evaporator, to be mixed again in an annular chamber underneath the core. Final heat-up to the envisaged core outlet temperature of 500°C was proposed to happen in a second superheater stage with upward flow again in assemblies at the core periphery. Assuming a hot channel factor of 2 for each heat-up step, as an initial guess, the power ratio of evaporator to superheater 1 to superheater 2 should be around 4:2:1 to reach the same peak coolant temperature in each region. The proposed core layout is trying to reach this power ratio by placing the second superheater at the core periphery where the neutron leakage is reducing the neutron flux anyway. Meanwhile, the concept has been worked out to a substantial detail to assess if the design target has been met.

2.3 Design Concept

A mechanical design of core components was worked out by Fischer et al. [7] which was updated recently by Koehly et al. [8] to account for the optimized moderator flow path indicated in Figure 1. Schulenberg et al. [9] summarize the basic features of the mechanical design and give a status of the first analyses performed for this concept. Some figures given here shall illustrate this design again to understand the following analyses.

A cut out view of a single fuel assembly is shown in Figure 2, left. The assembly box and the water box are made of a stainless steel sandwich construction with an internal honeycomb structure to improve the thermal insulation, as reported by Herbell et al. [10]. 40 fuel rods with 8 mm outer diameter are arranged with a pitch to diameter ratio of 1.18. A wire wrapped around each fuel rod with an axial pitch of 200 mm serves as a spacer providing efficient coolant mixing. The active core height of 4.2 m leads to a total core height of 5.331 m including inlet and outlet sections as well as a fission gas plenum.

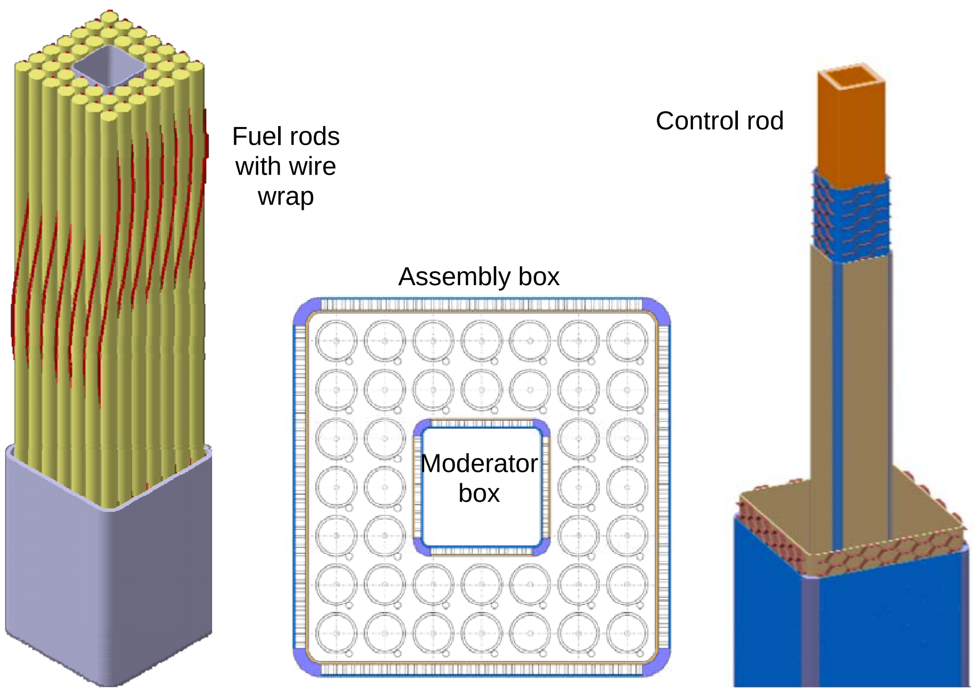

Figure 2 Assembly design with wire wrapped fuel rods (left) and honeycomb structures of the assembly and moderator box (right). A square control rod is inserted from top.

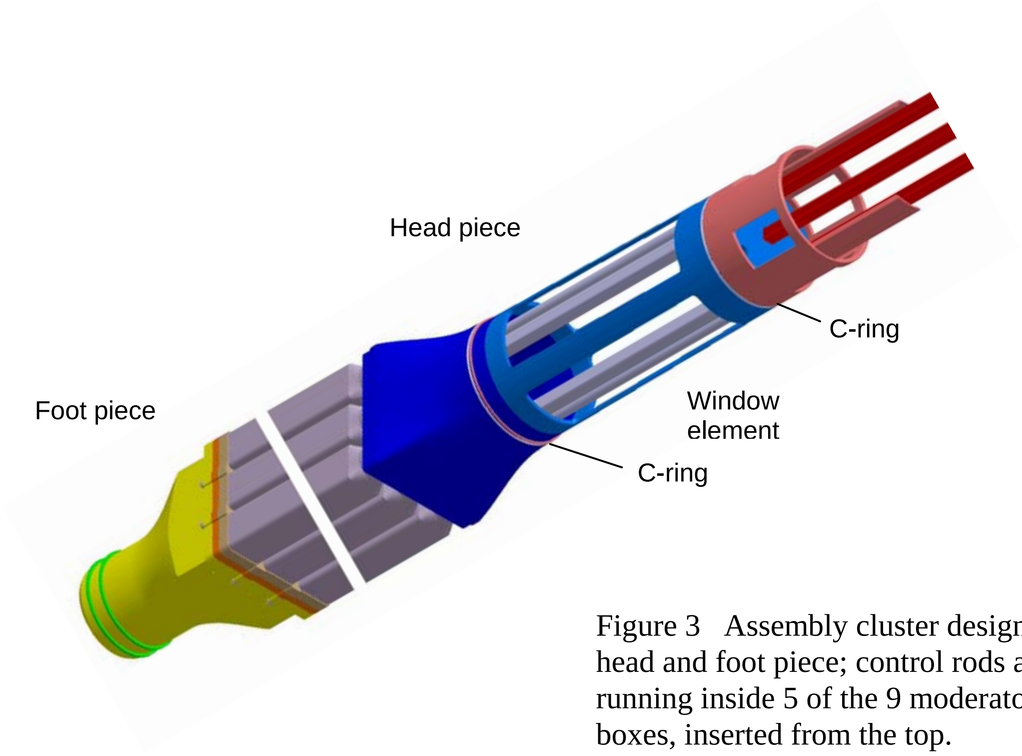

Figure 3 Assembly cluster design with head and foot piece; control rods are running inside 5 of the 9 moderator boxes, inserted from the top.

The arrangement of 9 of these assemblies to an assembly cluster with common head and foot pieces is illustrated in Figure 3. The moderator boxes are welded into the head piece, running through the upper mixing chamber and through the assemblies. Window elements in the head piece are releasing the steam horizontally at the evaporator or superheater 2 outlet. Inside the foot piece, a channel system is collecting all moderator water of each cluster to supply it to the gaps between the assembly boxes through horizontal openings in the foot piece. Square control rods, as proposed by Schlagenhaufer et al. [11], are running inside 5 of these water boxes as shown in Figs. 2 and 3. Inlet orifices avoid a mismatch between mass flow rates of moderator boxes with and without control rods. Two layers of spacer pads between assembly boxes are minimizing their bending as discussed by Schulenberg et al. [9].

3. Summary of Analyses Performed for the Thermal Core Design

Meanwhile, a large number of core design analyses have been completed to assess the feasibility [18]. The steady-state, full load power distribution of this core design has been analyzed in detail with coupled neutronic/thermal-hydraulic analyses for an equilibrium burn-up cycle. Local coolant and cladding temperatures were predicted with sub-channel and even with CFD analyses, and structural mechanics analyses were performed to yield deformations and stresses of core components [9]. The results enable to estimate the hot spot temperatures and the achievable burn-up and to quantify uncertainties as well as allowances for operation.

An equilibrium burn-up cycle has been predicted with KARATE and SPROD for this core, using up to 4 cycles of 1 year each. Different from conventional light water reactors, the new assembly clusters are not inserted at the outer core positions but rather at the outer positions of the evaporator region, whereas older assembly clusters are preferred in the superheater 2 region to achieve the envisaged power distribution. The pattern of clusters of different age is shown in Figure 4. The small upper numbers 4 and 6 refer to the cluster types used to replace the fuel as defined in Table 1. Solid lines separate evaporator from superheater clusters. Four fuel rods of each assembly have been doped with Gd for compensation of excess reactivity. The shuffling scheme and the control rod pattern are explained in [18].

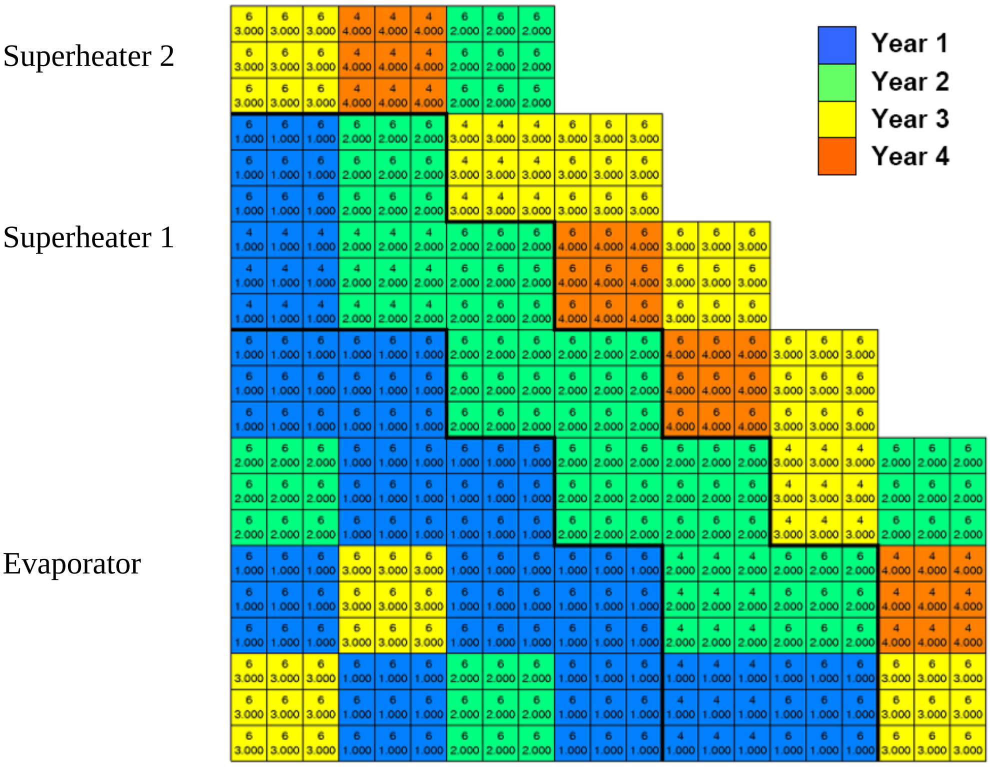

Figure 4 Age of assembly clusters in the equilibrium core

Cluster type	Axial segment	^{235}U Enrichment [w/o]			Gd_2O_3 content
		Basic	Corner	With Gd	
4	Bottom	6.0	5.0	5.5	2.0
	Top	7.0	6.0	6.5	2.0
6	Bottom	6.5	5.5	6.0	3.0
	Top	7.0	6.0	6.5	3.0

Table 1 Enrichment of assembly clusters to replace fuel

The assembly-wise radial burn-up distribution achieved at the end of the equilibrium cycle is shown in Figure 5. (The small upper numbers indicate the assembly number). Whereas some assemblies in the evaporator region are reaching a discharge burn-up of more than 50 GWd/t_{HM} at mid core height, the average discharge burn-up is only 32.5 GWd/t_{HM} which means that the design target has not yet been met.

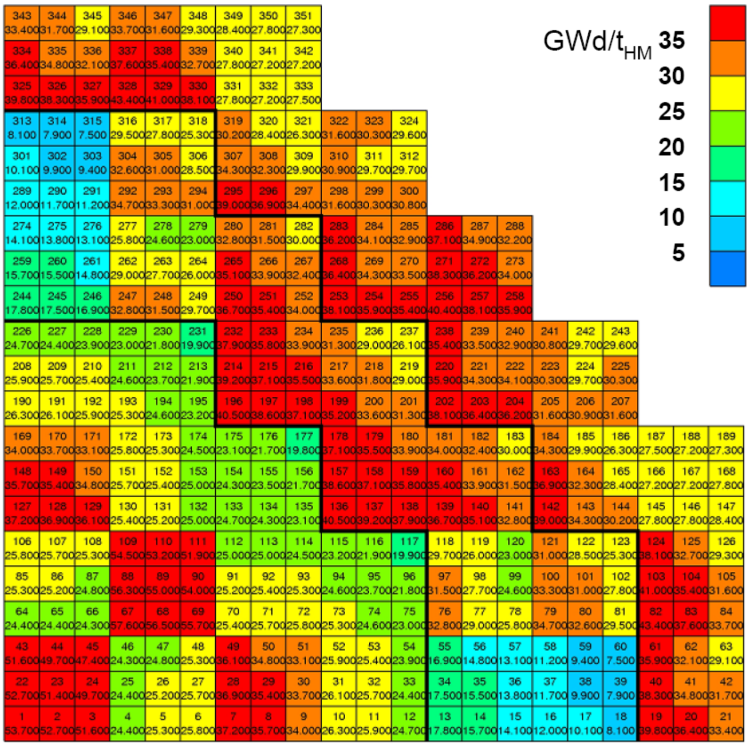

Figure 5 Burn-up distribution at the end of an equilibrium cycle at mid core height in GWd/t_{HM}

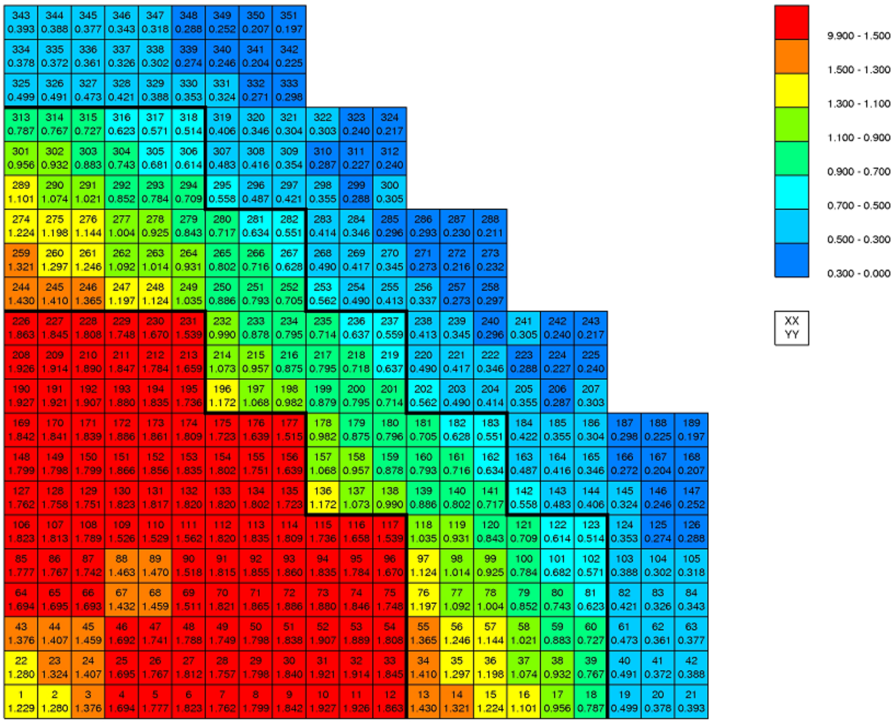

Figure 6 Assembly averaged, relative core power distribution at the end of an equilibrium cycle.

The core power distribution, shown exemplarily at the end of an equilibrium cycle in Figure 6, reflects the envisaged power split with the highest power in the evaporator region, where the coolant has still the largest margins from the target peak coolant temperature. The radial peaking factors within each heat-up step can be compensated to some extend by inlet orifices of the clusters, proving more coolant mass flow rate to clusters with higher power while restricting the mass flow of clusters with lower power. As an example, the coolant mass flow distribution at the end of an equilibrium cycle is shown in Figure 7. To simplify the design, however, inlet orifices for each individual assembly have not been considered yet in this design stage.

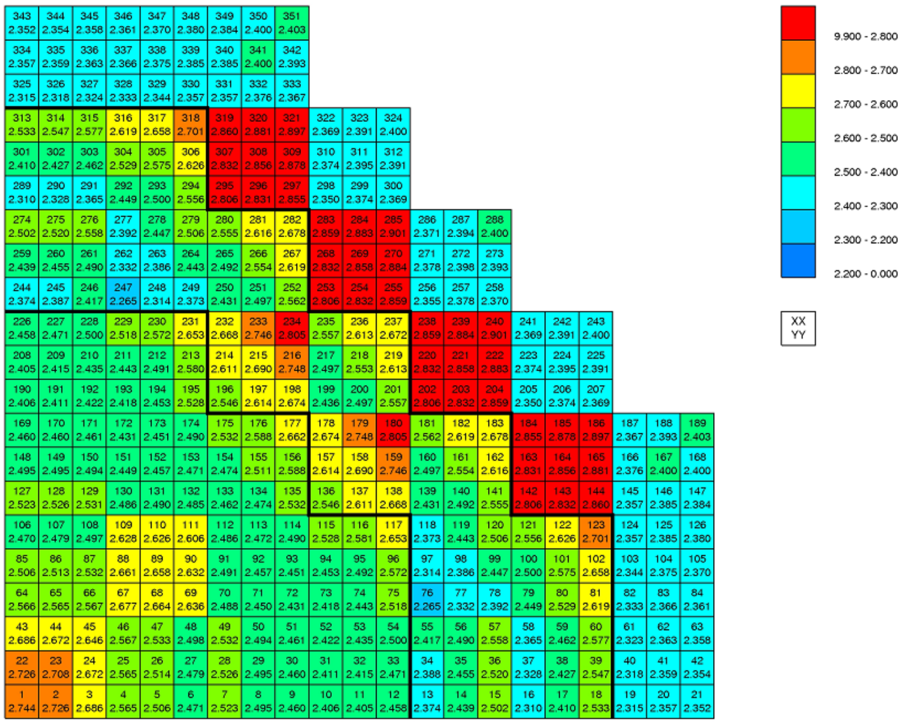

Figure 7 Coolant mass flow rate of assemblies in kg/s at the end of an equilibrium cycle.

The local power distribution of individual fuel rods inside each assembly is influenced by the radial flux gradient, which is largest in the superheater assemblies. Monti [12] succeeded to estimate the power of each fuel rod of the core by analyzing first the global flux distribution with the neutron transport code ERANOS coupled with the thermal-hydraulic code TRACE, which he multiplied then with the power distribution of a single assembly analyzed with MCNP5 for a given neutron flux. An exemplary analysis of such a pin power reconstruction technique has been performed for a core with fresh fuel of uniform enrichment, but its results can also be taken to estimate the local peaking factor of the core described above.

Further local power peaking factors arise from control rods which are inserted at the beginning of each equilibrium cycle to compensate the excess reactivity, from Gd poisoning of some fuel rods and its burn-out towards the end of the cycle, and from unavoidable deformations of assembly boxes. As examples of local power peaking factor analyses, we show in Figure 8 the change of the local power distribution of a single assembly cluster due to burn-up effects.

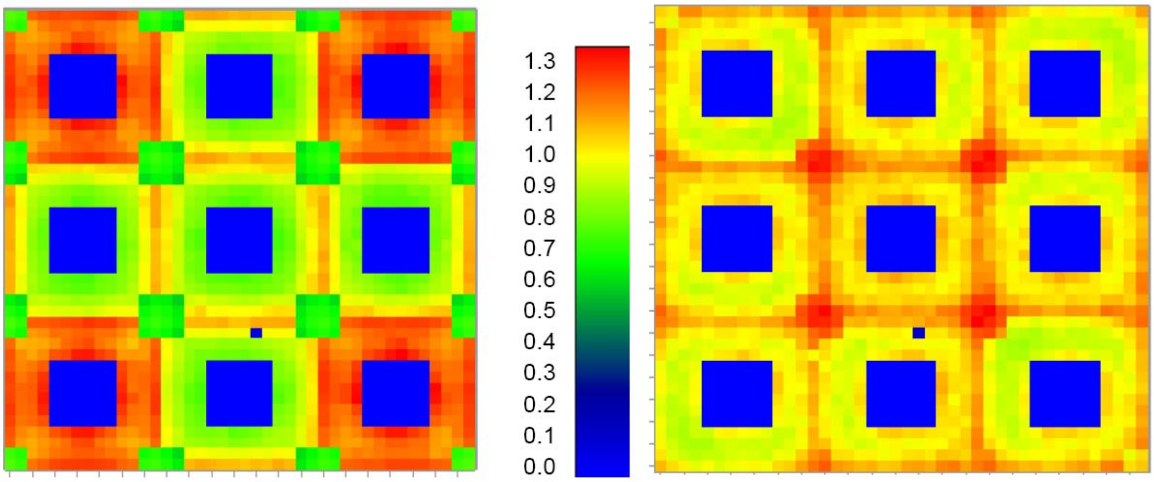

Figure 8 Local power peaking factors of an evaporator cluster with inserted control rods at the beginning of a burn-up cycle (left; corner rods contain 2.5% Gd_2O_3) and with Gd burn-out after a burn-up of 20GWd/t_{HM} (right; control rods extracted)

As a measure to manage the high enthalpy rise of the coolant in the core with such power peaking factors, an effective coolant mixing inside assemblies and between each heat up step has been a key requirement of this core concept. Mixing between sub-channels inside assemblies has been studied with sub-channel analyses by Himmel et al. [13]. A single wire wrapped around each fuel rod, which had already been applied successfully to sodium cooled fast breeder reactors in the past, turned out to be an effective mixing device which works well in both flow directions. It allows using the same assembly design in the evaporator as well as in both superheater sections. As a consequence of this mixing, even a radial power gradient of 20% inside a single assembly of superheater 2 caused only a coolant temperature non-uniformity of 25°C at the outlet, which corresponds to an enthalpy peaking factor of 1.12.

Coolant mixing in the upper and lower mixing chambers was studied by Wank [14] with the CFD code STAR-CD. The coolant enthalpy differences at the inlets of superheater 1 could be minimized by additional walls welded into the upper mixing chamber. Using the core power distribution as described above, Wank obtained a maximum enthalpy difference of around 45 kJ/kg at superheater 1 inlets. Similarly, mixing in the lower mixing chamber could be improved by adding swirl nozzles to the outlets of superheater 1 clusters in form of bended tubes welded with the core support plate. These swirl nozzles are causing a ring vortex in the lower mixing chamber which lower the enthalpy differences at superheater 2 inlets significantly. As a result, Wank [14] predicts there a maximum enthalpy difference of around 30 kJ/kg.

A large number of statistical uncertainties are contributing additionally to the peak coolant and peak cladding temperatures. Some of them were studied systematically during this project, like fuel rod displacements, partial blockage of a sub-channel, bending of assembly boxes and the uncertainties of codes taken for predictions. Starflinger et al. [18] discuss these uncertainties in more detail, concluding that an overall peaking factor of these statistical uncertainties of 1.2 will hardly be exceeded.

4. Hot Channel Assessment

The analyses summarized above lead to the following conclusions for the peak coolant outlet temperature of the hottest sub-channel of this core design.

In a first step, we derive the hot channel factors for coolant enthalpies. The radial peaking factors of assembly averaged coolant enthalpies throughout the equilibrium cycle are a consequence of the radial power form factors at beginning and end of cycle (BOC and EOC, resp.), divided by the coolant mass flow rate of each assembly. They range between 1.15 and 2.36 as shown in Figure 9, left.

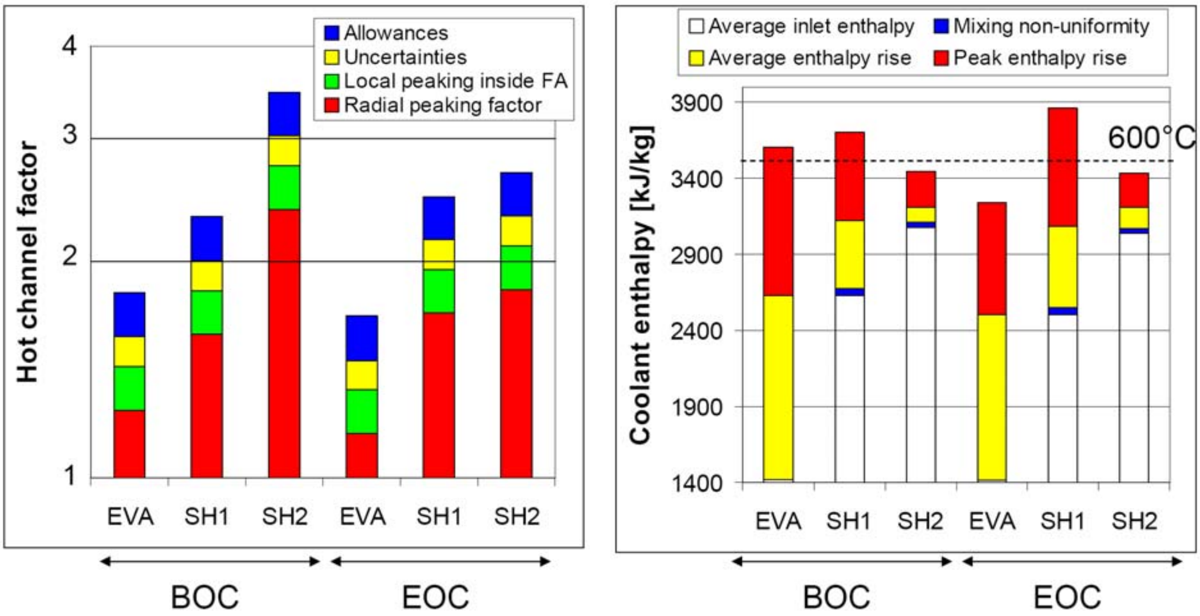

Figure 9 Hot channel factors (left) and coolant enthalpy rise (right) in the evaporator (EVA), the first superheater (SH1) and the second superheater (SH2) assemblies at beginning (BOC) and end (EOC) of an equilibrium burn-up cycle.

The local enthalpy peaking factors inside fuel assemblies are caused

- by the gradient of the neutron flux causing power peaking factors of individual fuel rods,
- by control rods and
- by Gd-poisoning of some fuel rods for compensation of excess reactivity.

While the local power peaking factors exceed even a factor of 1.3, as shown in Figure 8, most of these non-uniformities are mixed out in the coolant by the wire wrapped around the fuel rods. As a conclusion, we need to account for a local peaking factor of the coolant enthalpy of 1.15 only.

Uncertainties arise primarily

- from bending of assembly boxes, which is limited to max. 0.5 mm because of the spacer pads of these boxes as discussed by Schulenberg et al. [9],
- from uncertainties of neutronic and sub-channel codes and
- from local blockage of the coolant flow path.

We can assume that these uncertainties are statistical errors, so that they sum up rather as the sum of variances. In total, however, an uncertainty of 10% is not considered to be too conservative. Details are given in [18].

Finally, we need to account for allowance for operation and for the limited accuracy of the core and plant instrumentation. We assume a factor of 1.15 as a realistic guess, confirmed by first analyses of the control system by Schlagenhaufer et al. [5] and by a recent proposal for the core instrumentation by Koehly et al. [16].

If we multiply these coolant enthalpy peaking factors for each heat up step at BOC and EOC, we get the total peaking factors as shown in Figure 9, left. They range between 1.81 and 3.44 at BOC, decreasing to 1.68 and 2.66 at EOC. In superheaters, these peaking factors exceed the target hot channel factor of 2 mentioned in chapter 2.1, whereas the peaking factors in the evaporator have obviously some margin.

This result suggests to increase the power in the evaporator and to decrease it in the superheaters with respect to the envisaged power ratio of 4:2:1 (i.e. EVA 57%, SH1 29%, SH2 14%). The core design concept described here is following this strategy already to some extend. Figure 6 shows a power split of 62%, 30% and 8% at EOC, for EVA, SH1 and SH2, respectively.

The average coolant enthalpies at the inlet and outlet of each heat-up step, Figure 9 right, are a consequence of this power split. Due to the residual mixing non-uniformity of the upper and lower mixing chambers, the peak inlet enthalpy is slightly higher by up to 45 kJ/kg at SH1 inlet and up to 33 kJ/kg at SH2 inlet. From these data, the peak coolant enthalpies at the outlet of each heat up step can be estimated as the peak inlet enthalpies plus the total peaking factor times the average enthalpy difference.

Finally, the steam table yields the peak coolant outlet temperature for each peak outlet enthalpy. We get peak outlet temperatures beyond 600°C, which have obviously no more margin for the peak cladding temperature to stay below the material limits, in the evaporator and superheater 1 at BOC, and in superheater 1 at EOC, whereas the second superheater is not a cause for concern. Therefore, some further core optimization will be required to improve the remaining hot channels using the margins left in the rest of the core. The present result, however, is not too far from this optimum.

The peak fuel temperature is expected in the evaporator, where we predict a maximum linear heat rate of 39 kW/m at BOC decreasing to 32.5 kW/m towards EOC. The peak cladding surface temperature has been predicted by Monti [12] for a core with fresh fuel to be just 15°C hotter than the peak coolant temperature of the hottest sub-channel, since the hottest spots appear in the low power range of superheater 2. A detailed CFD analysis and component tests of the evaporator assemblies will be needed, however, to confirm these results, since Chandra et al. [17] predicted severe hot spots in a small scale evaporator assembly when they were searching for local effects of deteriorated heat transfer.

5. Conclusions

As a conclusion, most of the hot channel factors meet with the initial expectations of Schulenberg et al. [6], except the radial form factors in the superheater sections and the limited discharge burn-up. The main reason for both issues is the large size of the fuel assembly cluster. While the cluster design is appropriate in the evaporator region, where it enables a low form factor, easy fuel shuffling during revisions and standard control rod drives, the cluster size extends over the whole width of most of the superheater regions each. Thus, fuel shuffling from outside to inside, flattening the power profile, is disabled. Moreover, a compensation of enthalpy peaks by higher coolant mass flow rates in local superheater regions with higher power is disabled as long as the large assembly clusters can only be equipped with a common inlet orifice. Therefore, a recommendation for future design could be to control the inlet mass flow rate of each assembly individually. Another reason for the limited burn-up is the use of stainless steel which is more neutron absorbing than Zircalloy and a higher percentage of structural material than in conventional light water reactors.

The biggest uncertainties of this core design, however, are still caused by heat transfer predictions, in particular in evaporator region with high linear power, and by material properties of the stainless steel claddings. Some realistic fuel assembly tests will be needed to reduce these uncertainties to acceptable limits.

This paper highlights only some key results of the entire core design assessment. More details like stability limits, risks of flow reversal, linear power distribution, cladding temperatures, and more are given in [18].

6. Acknowledgments

This work has been funded by the European Commission as part of their project HPLWR-Phase 2, contract number 036230.

7. References

[1] J. Starflinger, T. Schulenberg, P. Marsault, D. Bittermann, C. Maraczy, E. Laurien, J.A. Lycklama, H. Anglart, N. Aksan, M. Ruzickova, L. Heikinheimo, "European Research Activities within the Project: High Performance Light Water Reactor Phase 2 (HPLWR Phase 2)", Proc. of ICAPP '07, Paper 7146, Nice, France, May 13-18, 2007.

[2] Y. Ishiwatari, M. Yamakawa, Y. Oka, S. Ikejiri, “Research and development of a Super Fast Reactor (1) Overview and High-Temperature Structural Design”, 16th Pacific Basin Nuclear Conference (16PBNC), Paper P16P1290, Aomori, Japan, Oct. 13-18, 2008.

[3] M. Brandauer, M. Schlagenhaufer, T. Schulenberg, “Steam cycle optimization for the HPLWR“, 4th International Symposium on Supercritical Water-Cooled Reactors, Paper No. 36, Heidelberg, Germany, March 8-11, 2009.

[4] K. Dobashi, Y. Oka, S. Koshizuka, “Conceptual design of a high temperature power reactor cooled and moderated by supercritical light water”, *Ann. Nucl. Energy* 25, 487-505, 1998.

[5] M. Schlagenhaufer, J. Starflinger, T. Schulenberg, “Steam cycle analyses and control of the HPLWR plant”, 4th International Symposium on Supercritical Water-Cooled Reactors, Paper No. 38, Heidelberg, Germany, March 8-11, 2009.

[6] T. Schulenberg, J. Starflinger, J. Heinecke, “Three pass core design proposal for a high performance light water reactor”, *Progress in Nuclear Energy* 50 (2008) 526-531

[7] K. Fischer, T. Schneider, T. Redon, T. Schulenberg, J. Starflinger, “Mechanical Design of Core Components for a High Performance Light Water Reactor with a Three Pass Core”, Proc. of GLOBAL 07, Boise, ID, USA, Sept. 9-13, 2007

[8] C. Koehly, T. Schulenberg, J. Starflinger, “Design concept of the HPLWR moderator flow path“, Proc. of ICAPP 09, Paper 9187, Tokyo, Japan, May 10-14, 2009

[9] T. Schulenberg, C. Maráczy, J. Heinecke, W. Bernnat, “Design and analysis of a thermal core for a HPLWR – a state of the art review“, Proc. NURETH-13, Paper N13P1039, Kanazawa, Japan, Sept. 27 –Oct. 2, 2009

[10] H. Herbell, S. Himmel, T. Schulenberg, “Mechanical Analysis of an Innovative Assembly Box with Honeycomb Structures Designed for a High Performance Light Water Reactor”, Proc. of IYNC 2008, Paper No. 132, Interlaken, Switzerland, Sept. 20 – 26, 2008.

[11] M. Schlagenhaufer, B. Vogt, T. Schulenberg, “Reactivity Control Mechanisms for a HPLWR Fuel Assembly”, Proc. of GLOBAL 07, Boise, ID, USA, Sept. 9-13, 2007

[12] L. Monti, “Multi-scale, coupled reactor physics/ thermal-hydraulics system and applications to the HPLWR 3 Pass Core”, Dissertation, *Karlsruhe Institute of Technology*, Karlsruhe, Germany (2009)

[13] S. R. Himmel, A.G. Class, E. Laurien, T. Schulenberg, “Sub-channel Analysis of a HPLWR Fuel Assembly with STAR-CD”, Proc. 16PBNC, Paper P16P1152, Aomori, Japan, Oct. 13-18, 2008

[14] A. Wank, “Fluid Dynamic Design of Complex Mixing Chambers”, Dissertation, *Karlsruhe Institute of Technology*, Karlsruhe, Germany (2009)

[15] T. Schulenberg, J. Starflinger, C. Maráczy, J. Heinecke, W. Bernnat, "Recent Analyses of the HPLWR Three Pass Core", Proc. ICAPP '10, Paper 10157, San Diego, CA, USA, June 13-17, 2010

[16] C. Koehly, W. Meier, J. Starflinger, "Integration of In-Core Instrumentation into HPLWR", ", Proc. ICAPP '10, Paper 10167, San Diego, CA, USA, June 13-17, 2010

[17] L. Chandra, J.A. Lycklama, D. C. Visser, "On the influence of wire-wrap spacer in a four rod-bundle cooled with supercritical water using CFD", Proc. NUTHOS-8, Paper N8P0062, Shanghai, China, Oct. 10-14, 2010

[18] J. Starflinger, T. Schulenberg, P. Marsault, D. Bittermann, E. Laurien, C. Maraczy, H. Anglart, J.-A. Lycklama, M. Andreani, M. Ruzickova, T. Vanttola, A. Kiss, M. Rohde, R. Novotny, "High Performance Light Water Reactor Phase 2, Public Final Report – Assessment of the HPLWR Concept", 6th Framework Programme, Contract No. FI60-036230, 2010, www.hplwr.eu